RF Photonics Signal Processing in Subcarrier Multiplexed Optical-Label Switching Communication Systems

Zuqing Zhu, *Student Member, IEEE, Student Member, OSA*, V. J. Hernandez, Min Yong Jeon, *Member, OSA*, Jing Cao, *Student Member, IEEE, Student Member, OSA*, Zhong Pan, *Student Member, IEEE, Student Member, OSA*, and S. J. Ben Yoo, *Senior Member, IEEE, Member, OSA*

***Abstract*—This paper provides theoretical and experimental studies of radio-frequency (RF) photonics processing techniques applicable in subcarrier-multiplexed optical-label switching (OLS) communications systems. The paper provides an overview of various label-coding technologies and introduces subcarrier multiplexing (SCM) as an attractive technology for OLS networks. All-optical-label extraction using optical filters, such as fiber Bragg gratings (FBGs), provides an effective means to demodulate the SCM labels without inducing RF fading effects caused by fiber dispersion. Furthermore, the role of fiber nonlinearities in the RF fading effects are theoretically and experimentally verified. The all-optical label extraction and rewriting processes constitute optical-label swapping, wherein 2R data regeneration can take place. Scalable and cascadable OLS systems are feasible by applying viable RF photonics technologies in all-optical-label processing.**

***Index Terms*—All-optical networks, fiber Bragg grating (FBG), fiber nonlinearity, label coding, optical Internet, optical-label swapping, optical-label switching (OLS), optical packet switching, RF fading, subcarrier multiplexing (SCM).**

I. Introduction

THE remarkable growth of Internet traffic has spurred research and development of scalable and high-capacity networking technologies. While the introduction of wavelength-division multiplexing (WDM) has provided increased capacity beyond 10 Tb/s over a single strand of fiber [1], improvements in switching capacity of Internet protocol (IP) routers have not been as impressive. Optical-label switching (OLS) [2] is a promising technology providing scalability in routing where switching occurs directly in the optical layer without optical–electrical–optical (O/E/O) conversions. The OLS network, realized on a WDM platform, utilizes a short ($\sim$ 40-b) optical label attached to a datagram to convey information pertaining to routing. Each OLS router (OLSR) reads the optical label, compares the label content with the routing table, makes a forwarding decision, and configures the switching fabric to forward the datagram to the desired output wavelength of the desired output port. Optical-label swapping in the OLSR provides network scalability beyond what can be sustained with a limited number of labels. A recently integrated OLSR has demonstrated a switching speed of 600 ps with 250-ns latency, with a prospect to scale beyond 42-Pbt/s switching capacity [3].

The architecture and the performance of the OLS network relies heavily on the methods used for encoding, transmitting, extracting, and rewriting the optical labels. Previous extraction methods [4] incorporating high-frequency electronics suffered from fading effects due to interactions between RF subcarrier waves and fiber dispersion [23]. Viable optical technologies for processing optical-subcarrier labels directly in the optical domain can be beneficial in many aspects. To this end, recent papers have proposed and demonstrated a number of new label encoding and decoding technologies [4]–[22]. This paper first compares these methods in Section II and determines that subcarrier multiplexing (SCM) is the most attractive method. Section III discusses SCM fiber transmission experimental results immune to RF fading effects. Section IV describes the interaction between this fading effect and fiber nonlinearities. Section V demonstrates all-optical label swapping technology with 2R data regeneration using SCM. Finally, Section VI concludes this paper.

II. Label-Coding Techniques

A key issue in the OLS approach is the method of coding the optical label onto a data payload, as it not only affects the architecture of the OLSRs but also strongly affects the performance of the OLS system. Recent research has proposed and demonstrated many label-coding techniques [4]–[22]. Among them, the four main approaches are 1) bit serial (time-division multiplexing), 2) label wavelength (WDM), 3) optical SCM, and 4) optical orthogonal modulation methods.

A. Bit-Serial Method

The bit-serial method utilizes time-division-multiplexed (TDM) labels [5]–[8], similar to the synchronous optical network/ synchronous digital hierarchy (SONET/SDH) overhead.

Manuscript received April 30, 2003; revised August 15, 2003. This work was supported in part by the Defense Advanced Research Projects Agency (DARPA) and Air Force Research Laboratory under Agreement F30602-00-2-0543; by the National Science Foundation under Grant ANI-998665; by Furukawa, Fitel, Sprint, and New Focus through gifts; and by the California MICRO program through matching funds.

Z. Zhu, V. J. Hernandez, J. Cao, Z. Pan, and S. J. Ben Yoo are with the Department of Electrical and Computer Engineering, University of California, Davis, CA 95616, USA (e-mail: yoo@ece.ucdavis.edu).

M. Y. Jeon was with the Department of Electrical and Computer Engineering, University of California, Davis, CA 95616, USA. He is now with the Chung Nam National University, Daejeon, Korea.

Digital Object Identifier 10.1109/JLT.2003.822237

The label and the payload are serial in the time domain, interspaced with an optical guard time to facilitate label extraction and processing. The bit rates of the label and the payload can be the same [6] or different [5]. This method is straightforward to implement at the transmitter end, since the label and the payload are both in baseband formats and use the same wavelength channel. It also provides possibilities for all-optical regeneration and label processing [6], [7]. However, the label receiving may require sophisticated synchronization and timing control [5]. In some cases, accurate control signals have to be generated at each hop to inform the label processors of the temporal positions of the labels [7]. In other cases, different power levels or coding formats (such as return to zero (RZ) and nonreturn to zero (NRZ)) are taken to distinguish the label and the payload [8]. Relatively complicated signaling or receiver designs make this bit-serial method difficult for practical applications. Moreover, the label and the data payload occupy separate time spaces, limiting the available data throughput.

B. Label Wavelength Method

The label wavelength method transmits the optical label on one [9] or multiple [10] wavelength channels that are transmitting the optical labels. The label extracting and swapping is easily achieved by using separate optical transceivers for the label and the payload occupying separate wavelengths. The primary drawback results from the chromatic dispersion of the optical fiber. Different wavelength channels propagate through the fiber at different speeds, resulting in walk-off between the label and the payload. This phenomenon limits the transmission distance and the network scalability, unless each link incorporates dispersion management. Limited network scalability is also an issue. Allocating one label wavelength for each payload channel will clearly require a far greater optical bandwidth than required by the information on the label and the data. Allocating one label wavelength for all of the multiple payload channels [9] could cause collisions between labels the traffic becomes heavy. Furthermore, this method greatly underutilizes the label channel capacity since the optical labels are relatively short and low speed compared with the data payloads.

C. Optical SCM Method

The optical SCM technique [4], [11] places the label in-band in terms of the wavelength channels, but out-of-band in terms of the modulation channels. It accommodates both the label and the data payload on the same optical wavelength by treating the payload as a baseband signal while modulating the label on the subcarrier channels [4], [11]. Fig. 1 shows the SCM-labeled signal in the time and frequency domains. The SCM label does not occupy any additional time slot but instead occupies a small amount of additional bandwidth (100 MHz–1 GHz) in the optical spectrum. Using the SCM method, the label and the payload travel simultaneously through the network, and there is no need to maintain tight synchronization at any node, achieving simplified network control. Furthermore, the SCM labeling method is relatively efficient in terms of wavelength channel utilization in that the SCM labels do not occupy any additional time slots or wavelength channels. The additional bandwidth required is usually well within what

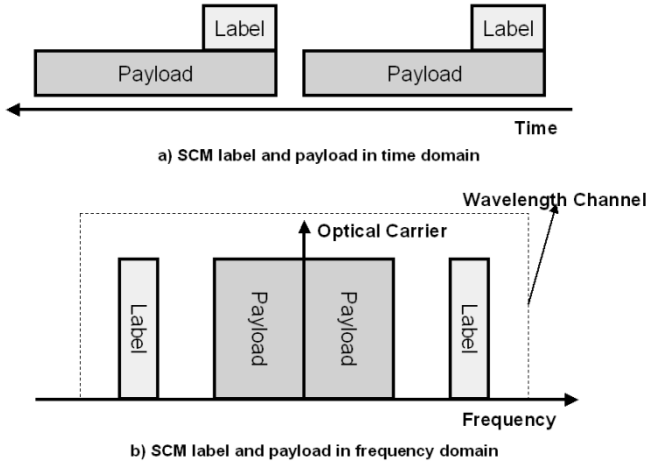

Fig. 1. SCM label and payload in (a) time domain and (b) frequency domain.

can be accommodated between the channel spacing of the dense-wavelength-division-multiplexing (DWDM) networks. There are methods to even further improve the channel utilization of SCM labeling, such as single-sideband (SSB) transmission [12] and dispersion-division multiplexing [13]. As this paper discusses in later sections, the SCM labeling method also allows flexible label extraction and swapping in the optical domain. While the main drawback of the SCM technique is the RF fading effect coming from the interaction between the RF subcarrier and the chromatic dispersion in optical fibers [14], the optical-frequency-domain filtering method eliminates the fading effects [15]. Section III discusses this technique in detail.

D. Orthogonal Modulation Method

The orthogonal modulation technique encodes the optical-label information using the optical carrier itself [22]. The data payload is intensity modulated, while the label is represented by either the phase [18] or the frequency [16], [17] information of the optical carrier. For example, in the amplitude shift- keying (ASK) payload/frequency shift-keying (FSK) label scheme, the label frequency modulates the optical carrier first, using one optical frequency f_0 to transmit "0" and another optical frequency f_1 for "1", and then the payload modulates the intensity of the FSK carrier. In the label receiver, an optical bandpass filter removes the signal light at f_0, and a photodetector and an electrical low-pass filter demodulate the label from the filtered light. The payload receiver uses a photodetector to convert the intensity-modulated payload into an electrical signal and to remove the FSK label. This novel technique allows all-optical label swapping, flexible wavelength conversion, and high-bit-rate operation [19]. This scheme is limited by the extinction ratio of the payload, which cannot exceed a certain limit [20], [21]; otherwise, the orthogonal modulation scheme will lose the label information. There is a tradeoff between the signal qualities of the payload and the label. This requirement limits the system transparency to the signal format and introduces crosstalk. Fiber dispersion and nonlinearities also affect this label-coding method. For FSK-based orthogonal modulation, the two FSK

TABLE I
COMPARISON OF THREE MAIN APPROACHES OF LABEL CODING

Label coding methods	Timing requirement	Crosstalk	Label Processing
Bit serial	Tight, it requires synchronization control of the label and the payload.	Very low, the label and the payload are separated in the time domain.	All-optical label processing is feasible.
Label wavelength	Loose, the label and the payload can be overlapped in the time domain and the processings of them do not require accurate synchronization.	Very low, the label and the payload occupy different wavelength channels and take different optical transceivers.	Separate label transceivers simplify label processing.
Optical SCM	Loose, the label and the payload are overlapped in the time domain and they can be processed asynchronously.	Low, but it may suffer from RF fading effect, depending on the label detection method.	Experiments demonstrated label swapping [26-27] and contention resolution [25].
Orthogonal modulation	Loose, the label and the payload are overlapped in the time domain and they can be processed asynchronously.	High	All-optical label swapping is feasible [28] but with low signal quality.

tones with large tone spacing will have different responses when propagating through the fiber, distorting the payload signal and increasing crosstalk. For high-bit-rate differential phase-shift-keying (DPSK) label, the fiber dispersion and nonlinearity will affect the phase information of the optical carrier and deteriorate the signal. While the fiber dispersion may not limit the performance for relatively low-bit-rate (<1 Gb/s) DPSK labeling, the DPSK modulation may impose stringent requirements on the linewidth of the laser (>10 MHz) [21].

E. Overall Comparison

Table I summarizes overall discussions on the label-coding schemes. The optical SCM technique shows a number of attractive properties, including high wavelength channel utilization, a loose timing requirement, low crosstalk, and flexible label extracting and rewriting. In the following two sections, this paper discusses theoretical and experimental studies of optical-label extraction, fiber transmission including nonlinear optical effects, and label swapping.

III. OPTICAL SCM THEORY

Simple optical amplitude modulations of the RF subcarrier result in two sidebands around the optical carrier. During the propagation of this double sideband (DSB) signal through a dispersive fiber, the upper and the lower SCM sidebands will undergo different phase shifts due to the different phase velocities. The square-law photodetection applied to this DSB signal will exhibit the RF fading effect, which comes from the interaction of the optical carrier and the two SCM sidebands.

A. Small-Signal Analysis

The intensity of a light signal with the encoded payload and the SCM label has the expression

$$I(t) = I_0[P(t) + mL(t)\cos(\omega_s t)] \tag{1}$$

where $P(t)$ and $L(t)$ are the amplitude of the payload and the label, m is the modulation index of subcarrier label, and ω_s is the angular frequency of the subcarrier. The light signal in (1) will suffer from the RF fading effect after propagating through a dispersive fiber and being recovered by a photodiode. To analyze this phenomenon analytically, we perform a small-signal approximation [24]. The small-signal model assumes that there is no modulation on optical baseband and SCM channels, and the amplitude of the subcarrier is smaller than that of the optical carrier. This model reduces the light intensity in (1) to a small-signal formula [24]

$$I = I_0(1 + m\cos(\omega_s t)) \tag{2}$$

where m is the modulation index and $m < 1$. Equation (2) shows that I_0 represents the amplitude (information) of the optical baseband signal (payload channel), and $I_0 m$ represents the

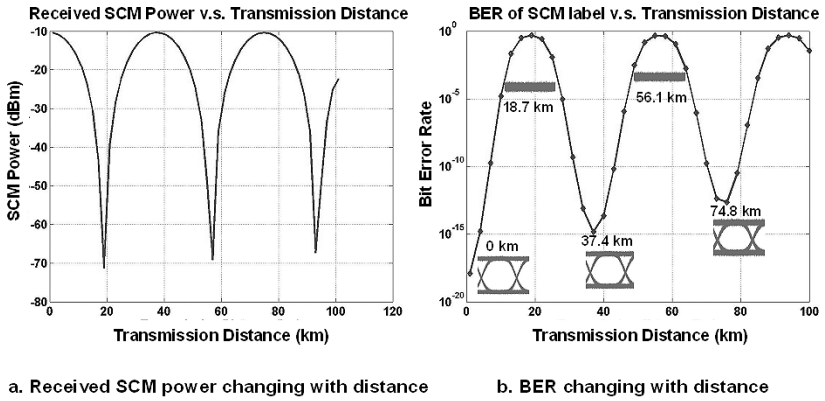

Fig. 2. Simulation of RF fading effect: (a) received SCM power changing with distance, and (b) bit-error rate (BER) changing with distance (insets are the eye diagrams of the recovered label signal at different distances). (Simulations ignore optical losses during the fiber transmission.)

amplitude (information) of the optical SCM signal (SCM label channel). The electric field of the light signal is a periodic function in time, and it can be decomposed into a Fourier series [24]

$$E = \exp(j\omega_0 t) \sum_k A_k \exp(jk\omega_s t) \tag{3a}$$

$$E = \sqrt{I_0}\left[1 + \frac{1+j\alpha}{4} m \exp(j\omega_s t) + \frac{1+j\alpha}{4} m \exp(-j\omega_s t) + j\frac{\alpha}{16} m^2 \exp(j2\omega_s t) + j\frac{\alpha}{16} m^2 \exp(-j\omega_s t) + \cdots\right] \tag{3b}$$

where ω_0 is the optical carrier frequency, and α is the chirp parameter of the light source. As illustrated in (3b), the signal power is mainly distributed in the three components restricted to the first power of m when $m < 1$. For the cases that $m > 1$, it is necessary to take the high-order components into account. The Fourier coefficients of the three dominant components are [24]

$$\begin{aligned} A_{-1} &= \sqrt{I_0} m \frac{1+j\alpha}{4} \\ A_0 &= \sqrt{I_0} \\ A_1 &= \sqrt{I_0} m \frac{1+j\alpha}{4}. \end{aligned} \tag{4}$$

In (4), we can recover I_0 from A_0 and recover $I_0 m$ from A_{-1} and A_1; thus, A_0 represents the information of the payload channel, while A_{-1} and A_1 represent the information of the SCM label channel. During the propagation on a dispersive fiber, those three components have slightly different phase velocities and acquire different phase shifts at the receiver. Define those phase changes as ϕ_{-1}, ϕ_0, and ϕ_{+1}. Then, the electric field of the light signal after propagating through a dispersive medium is [24]

$$E = \exp(j\omega_0 t) \sum_{k=-1}^{1} A_k \exp(j(k\omega_s t + \phi_k)). \tag{5}$$

In the angular frequency domain, this electrical field is

$$E(\omega) = A_{-1}\exp(j\phi_{-1})\delta(\omega - (\omega_0 - \omega_s)) + A_0 \exp(j\phi_0) \times \delta(\omega - \omega_0) + A_{+1}\exp(j\phi_{+1})\delta(\omega - (\omega_0 + \omega_s)) \tag{6}$$

where $\delta(\omega)$ is the impulse function. In (6), there are three carriers (an optical carrier and two SCM sidebands) with different phase shifts, and they will interact with each other in a photodiode to generate two subcarrier components with different phases in the received electrical signal [24]. The phase difference between the two components will vary with the transmission distance. Thus, the total power of these two components will fluctuate over different transmission distances. This analysis ignores the optical losses in the fiber, since it contributes only for a constant factor in the frequency response. At the receiver, the photocurrent generated by the photodetector is given as $i = (1/2)\rho E E^*$ (ρ is the responsivity of the photodiode), and the received SCM signal power is [23]

$$P_{SCM} \propto \cos\left[\pi L c D \left(\frac{\omega_s}{\omega_0}\right)^2 + \arctan(\alpha)\right]. \tag{7}$$

Equation (7) shows that the received SCM signal power will be changing with the transmission distance if all the other parameters are fixed. This is the RF fading effect of the optical SCM systems. The received SCM power will be zero at the distances [23], [24]

$$L = \frac{1}{2}\left(\frac{\omega_0}{\omega_s}\right)^2 \frac{1}{Dc}\left[2N + 1 - \frac{2}{\pi}\arctan(\alpha)\right], \quad \text{where } N = 0, 1, 2, \ldots. \tag{8}$$

In the 1550-nm range, a single-mode fiber (SMF) has $D = 17$ ps/(nm $*$ km). At 14-GHz subcarrier frequency, those distances are

$$L = \left[2N + 1 - \frac{2}{\pi}\arctan(\alpha)\right] * 18.7 \text{ km}, \quad \text{where } N = 0, 1, 2, \ldots. \tag{9}$$

At these transmission distances, the RF fading effect will cancel out the SCM label signal. Simulation results manifest this phenomenon. Fig. 2 shows the simulation results assuming zero-chirp modulation. In the simulation, we ignore the optical loss of the fiber but decrease the optical signal-to-noise-ratio with the distance; by doing this, we simulate a steady-state fiber link with distributed optical amplifiers. As small-signal analysis predicted in (9), the received SCM power reaches to a minimum for approximately every 38 km. At $L = 18.7$ and 56.1 km, the eyes close, and only the noise appears.

The RF fading effect limits the system's transparency to transmission distance. While dispersion-compensated transmission links are widely used today, the frequency chirp in optical

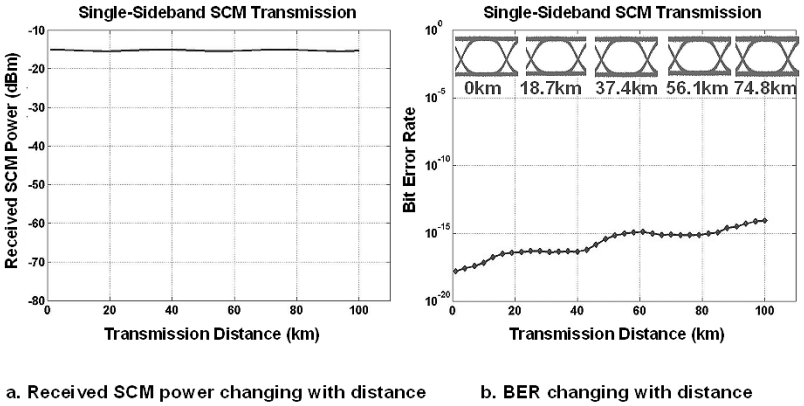

Fig. 3. Simulation results of SSB-SCM transmission: (a) received SCM power changing with distance, and (b) BER changing with distance (insets are the eye diagrams of the recovered label signal at different distances). (Simulations ignore optical losses during the fiber transmission.)

SCM signals rising given modulation characteristics can still induce fading. The frequency chirp of the optical transmitter is usually difficult to predict at the receiver, and it is difficult to cancel by dispersion compensation. Thus, it is desirable to find methods that do not require any knowledge about the optical transmitter to eliminate the RF fading effect. Optical spectral filtering may satisfy this requirement. There are two options: one is SSB transmission [30] and the other is carrier-suppressed label extraction [15]. Both methods may benefit from suitable optical filters, such as fiber Bragg gratings (FBGs) [15].

An FBG functions as an optical bandpass filter for the reflected field and an optical band-stop filter for the transmitted field [29]. Assuming that the FBG has a Gaussian-shape frequency response and the amplitude response for the reflected field is given as

$$H(\omega) = \exp\left(-B\left(\frac{(\omega-\omega_c)}{\Delta\omega}\right)^2\right) \tag{10}$$

where ω_c is the center frequency of the FBG, $\Delta\omega$ is the 3-dB bandwidth, and $B = 0.3466$ is a constant. The reflected field results from multiplying (6) by (10) given as

$$\begin{aligned} E_r(\omega) = E(\omega)H(\omega) &= A_{-1}\exp(j\phi_{-1}) \\ &\cdot \exp\left(-B\left(\frac{(\omega_0-\omega_s-\omega_c)}{\Delta\omega}\right)^2\right)\delta(\omega-(\omega_0-\omega_s)) \\ &+ A_0\exp(j\phi_0)\exp\left(-B\left(\frac{(\omega_0-\omega_c)}{\Delta\omega}\right)^2\right)\delta(\omega-\omega_0) \\ &+ A_{+1}\exp(j\phi_{+1})\exp\left(-B\left(\frac{(\omega_0+\omega_s-\omega_c)}{\Delta\omega}\right)^2\right) \\ &\times \delta(\omega-(\omega_0+\omega_s)). \end{aligned} \tag{11}$$

Equation (11) shows that the FBG multiplies a constant coefficient onto each of the three frequency components in (6), and the coefficients' values are determined by ω_c and $\Delta\omega$. Thus, by carefully adjusting ω_c and $\Delta\omega$, one can suppress one or two of the SCM sidebands with an FBG.

B. SSB-SCM Transmission

Suppose the SSB transmitter removes the upper SCM sideband ($A_1\exp(j(\omega_0+\omega_s)t)$ in (5)); then, the electrical field of the light signal after fiber transmission is

$$E = \exp(j\omega_0 t)[A_{-1}\exp(j(-\omega_s t+\phi_{-1})) + A_0\exp(j\phi_0)] \tag{12}$$

where ϕ_0 and ϕ_{-1} are the phase shifts that are defined in (5). At the receiver, the photodetector generates a photocurrent proportional to the intensity of the optical signal and the photocurrent is given as

$$\begin{aligned} i = \frac{1}{2}\rho EE^* &= \frac{1}{2}\rho\left[|A_{-1}|^2+|A_0|^2\right. \\ &+A_{-1}A_0^*\exp(j(-\omega_s t+\phi_{-1}-\phi_0)) \\ &\left.+A_{-1}^*A_0\exp(j(\omega_s t-\phi_{-1}+\phi_0))\right] \\ &= \frac{1}{2}\rho\left[|A_{-1}|^2+|A_0|^2+2\mathrm{Re}(A_{-1}A_0^*)\right. \\ &\left.\cdot\cos(\omega_s t-\phi_{-1}+\phi_0)\right] \end{aligned} \tag{13}$$

where ρ is the responsivity of the photodiode. Only one component with frequency ω_s exists in this received electrical signal, and the RF fading term disappears. Simulation results also prove this result. In Fig. 3(a), the received SCM signal power is almost the same for different distances after SSB transmission. The small BER fluctuation in Fig. 3(b) is caused by the nonideal SSB-SCM generation, or in other words, the optical filter cannot totally remove the lower SCM sideband, and the remainder of it causes the fading-like small BER fluctuation.

Fig. 4 shows the SSB transmission experimental setup. The setup consists of a distributed feedback (DFB) laser diode (DFB-LD), a Mach–Zehnder modulator (MZM), an erbium-doped fiber amplifier (EDFA) with bandpass filter, an optical circulator, an FBG, a $0 \sim 80$ km transmission SMF, and a label detector. The 10-Gb/s MZM is driven by the combined signal of the data payload and the SCM label. The payload signal is 2.5-Gb/s NRZ format with $2^{31}-1$ pseudo-random binary sequence (PRBS), and the SCM label signal is 155-Mb/s NRZ ASK-modulated signal with $2^{31}-1$ PRBS on a 14-GHz RF subcarrier. The center wavelength of the DFB LD

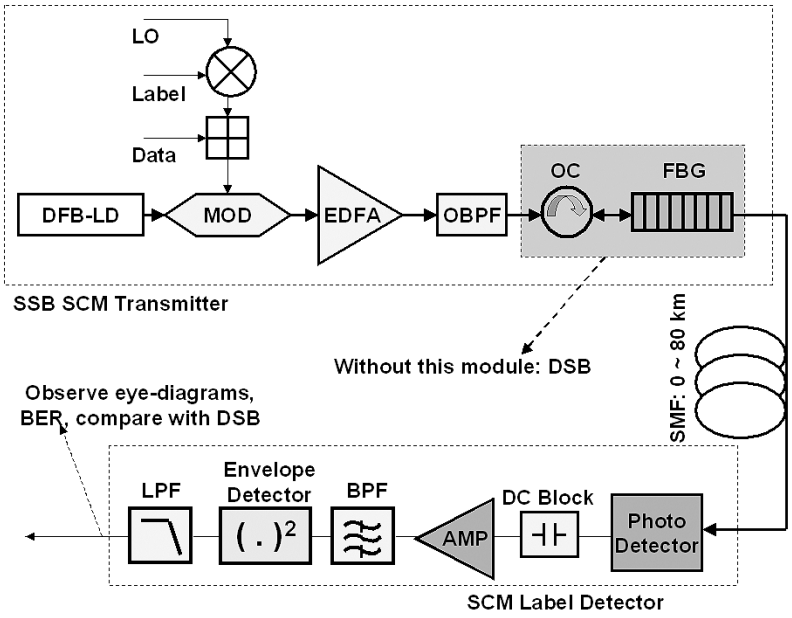

Fig. 4. Experimental setup for the fiber transmission using the SSB-SCM signal. DFB-LD: DFB laser diode; LO: electrical local oscillator; Mod: optical modulator; OBPF: optical bandpass filter; SMF: single-mode fiber; OC: optical circulator; FBG: fiber Bragg grating; LPF: electrical low-pass filter; AMP: RF amplifier; BPF: electrical bandpass filter.

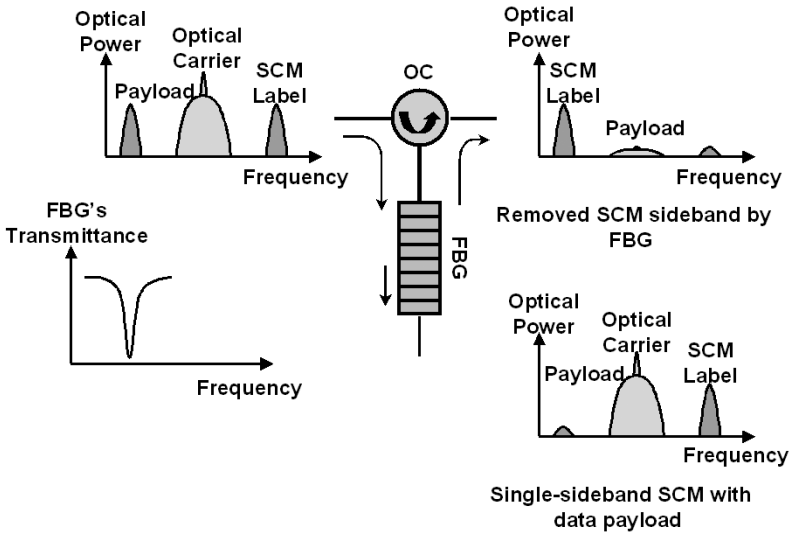

Fig. 5. Generation of the SSB-SCM signal. OC: optical circulator; FBG: fiber Bragg grating.

is 1557.36 nm. As Fig. 5 illustrates, the SSB-SCM generation involves the amplified DSB-SCM signal entering the optical circulator and the FBG and subsequently being filtered by the FBG with peak reflectivity centered at 1557.25 nm to reject one SCM sideband. The photodiode conducts an optical–electrical (O/E) conversion of the SSB-SCM signal after fiber transmission, and the electrical bandpass filter and the envelope detector recover the 155-Mb/s label from the received electrical signal.

The right-hand side inset of Fig. 4 shows the structure of the SCM label detector. It consists of a dc block, a low-pass filter, a bandpass filter, an envelope detector, and an amplifier. The experiment included measurements of the BER performance for both of the SSB-SCM and DSB-SCM labels, over 10–80-km SMF transmission. Fig. 6 shows the label receiver sensitivity (at 1E-9 BER level) measurements for both of the SSB-SCM and DSB-SCM schemes,over 0–80-km SMF transmissions. The insets are the received label eye diagrams measured at each transmission length. The DSB-SCM scheme shows significant signal deterioration owing to fading effects around 20 and 60 km, while the label eye diagrams of the SSB-SCM scheme show clear eye openings at different transmission distances. The SSB-SCM signal does not suffer from the RF fading effects.

C. Carrier-Suppressed DSB-SCM Label Extraction

Optical carrier suppression is another method to eliminate the RF fading effect [15]. Fig. 8 shows a configuration of carrier-suppression DSB-SCM. The FBG acts as a demultiplexer

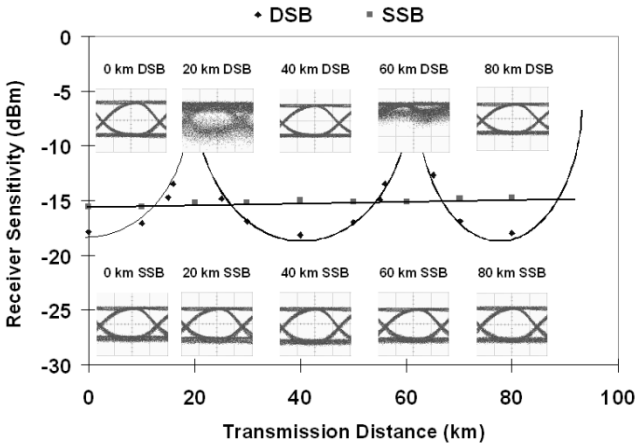

Fig. 6. Receiver sensitivity verus transmission length for DSB and SSB label modulations.

to optically separate the label and the payload before the photodetector. In this scheme, the electrical field of the light signal after FBG is

$$E = \exp(j\omega_0 t)[A_{-1}\exp(j(-\omega_s t + \phi_{-1})) + A_{+1}\exp(j(\omega_s t + \phi_{+1}))]. \tag{14}$$

Then, the photodetector's output current is

$$\begin{aligned} i &= \frac{1}{2}\rho\left\{|A_{-1}|^2 + |A_{+1}|^2 + A_{-1}A_{+1}^* \right. \\ &\quad \cdot \exp(j(-2\omega_s t + \phi_{-1} - \phi_1)) + A_{+1}A_{-1}^* \\ &\quad \left. \cdot \exp(j(2\omega_s t + \phi_1 - \phi_{-1}))\right\} \\ &= \frac{1}{2}\rho\left\{|A_{-1}|^2 + |A_{+1}|^2 + 2\mathrm{Re}(A_{-1}A_{+1}^*) \right. \\ &\quad \left. \cdot \cos(2\omega_s t + \phi_1 - \phi_{-1})\right\}. \end{aligned} \tag{15}$$

An electrical low-pass filter then filters out the $2\omega_s$ component. Finally, the received signal only contains the label information, and the RF fading term disappears. Fig. 7 shows simulation results in which the received label signal power is constant and eyes are always open, regardless of the transmission distance. Fig. 9 shows the experimental setup for measuring the fading effects. The label detector consists of an optical circulator, an FBG, a photodetector, and an electrical low-pass filter. Fig. 10 shows the relation between the receiver sensitivity (at 1E-9 BER level) and the transmission length. The experiment results prove that the FBG-based label extraction effectively suppressed RF fading effects. The optical loss in the fiber causes the receiver sensitivity to increase with the transmission distance.

IV. Nonlinear Optical Effects and RF Fading

As described in the previous formulas, the fiber dispersion causes the RF power of a DSB-SCM signal to vary as a function of fiber distance. These derivations assume that the optical powers are small enough to neglect nonlinear optical effects, which cannot be ignored when fiber amplifiers are used in the link. In reality, the DSB-SCM signal strength varies as a function of the input optical power, and this section explores the effects of the fiber nonlinearities on the DSB-SCM signal transmission. This section includes small-signal analyses to predict the mathematical behavior of the fading, followed by simulations and experimental results to show the true behavior of the subcarrier.

A. Small-Signal Analysis

One can analyze the effects on nonlinearities by using the small-signal approach [24] used in Section III-A. This assumes that the intensity I undergoes small-signal modulation ((2)) and that the field E can be expressed as a Fourier series ((3)). The baseband and subcarrier components are represented by (4). After propagation through the fiber, the field components experience the phase change ϕ_k, which represents phase induced by dispersion and nonlinearities [24]

$$E = \exp(j\omega_0 t)\sum_{k=-1}^{1} A_k \exp(j(k\omega_s t + \phi_k)) \tag{15}$$

$$\phi_k = -\beta_k L + \gamma |A_k|^2 L_e. \tag{16}$$

In ϕ_k, there are two components—the dispersion term and nonlinear term. Fiber attenuation must be considered in the nonlinear term, but a separate fiber attenuation term is excluded in ϕ_k, since it is uniform for all k. In the dispersion term, L is the fiber propagation length, and β_k is the propagation constant. In the nonlinear term, γ is the nonlinear coefficient, and L_e is the effective length of the fiber. The effective length is the distance over which the nonlinearity affects the field and is defined as

$$\begin{aligned} L_e &= \frac{1 - e^{-\alpha_L L}}{\alpha} \\ \alpha_L &= -\frac{\alpha_{L\ \mathrm{dB}} \ln 10}{10}. \end{aligned} \tag{17}$$

α_L describes the fiber loss per kilometer, and $\alpha_{L\ \mathrm{dB}}$ is the loss in units of decibels, neither of which should be confused with the chirp parameter a. The intensity component of frequency ω_s ($k = 1$) received by the photodetector is given by

$$\begin{aligned} I &= EE^* \\ &= \frac{1}{2}\Re\left(A_1 A_0^* e^{j(\beta_0 L - \beta_1 L + \gamma|A_1|^2 L_e - \gamma|A_0|^2 L_e)} \right. \\ &\quad \left. + A_0 A_1^* e^{-j(\beta_0 L - \beta_1 L + \gamma|A_1|^2 L_e - \gamma|A_0|^2 L_e)}\right). \end{aligned} \tag{18}$$

Inserting (4) into (18) yields the following RF sideband power, where the power can be directly substituted for intensity. It assumes $m \ll 1$, as follows:

$$P_f = P_0 m\sqrt{1+\alpha^2}\left|\cos\left\{\frac{\pi\lambda^2 DLf_s^2}{c} + \arctan(\alpha) - \gamma P_0 L_e\right\}\right| \tag{19}$$

where f_s is the subcarrier frequency in hertz.

The minimum RF powers occur for

$$\frac{\pi\lambda^2 DLf_s^2}{c} + \arctan(\alpha) - \gamma P_0 L_e = \frac{\pi}{2} + \pi n. \tag{20}$$

Solving for the null frequency yields an expression that allows one to predict the behavior of the fading as a function of power, chirp, and dispersion, as follows:

$$f_s = \sqrt{\frac{c}{\lambda^2 DL2}\left(1 + 2n - \frac{2}{\pi}\arctan(\alpha) + \frac{2\gamma P_0 L_e}{\pi}\right)}. \tag{21}$$

From this equation, one finds that the chirp parameter roughly provides an overall shift in the null frequency. The power will

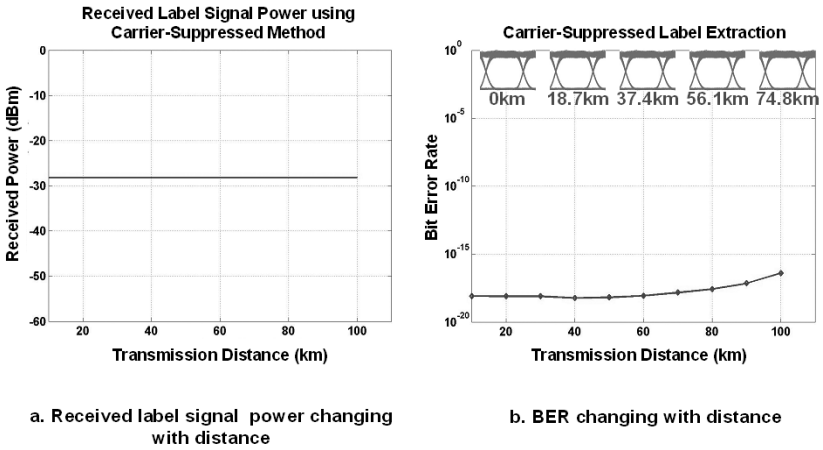

a. Received label signal power changing with distance

b. BER changing with distance

Fig. 7. Simulation results of carrier-suppressed method: (a) received label signal power for different distances, and (b) BER results and eye diagrams.

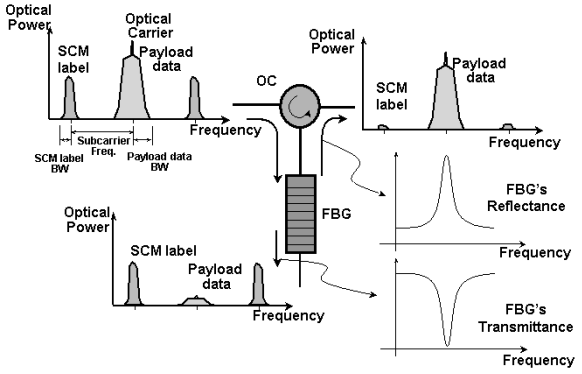

Fig. 8. Optical carrier suppression and subcarrier label extraction using an FBG. OC: optical circulator; FBG: fiber Bragg grating.

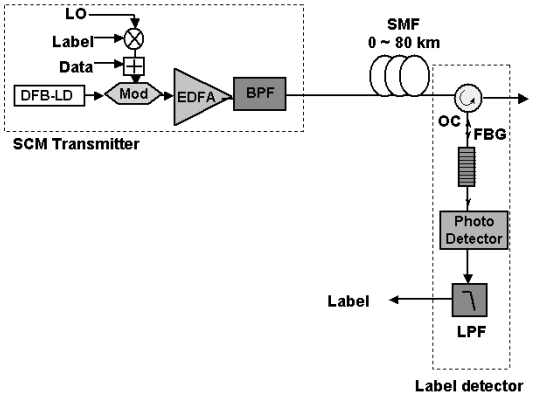

Fig. 9. Experimental setup of label extraction with FBG. DFB-LD: DFB laser diode; LO: electrical local oscillator; Mod: optical modulator; BPF: optical bandpass filter; SMF: single-mode fiber; OC: optical circulator; FBG: fiber Bragg grating; LPF: electrical low-pass filter.

also shift the null frequency, but it only becomes significant when P_0 becomes greater than the nonlinear factor $\pi/2\gamma L_e$. From (20), it would also be convenient to solve for an expression that describes the distance L for a given subcarrier frequency, but a closed-form expression for L does not exist. In the next

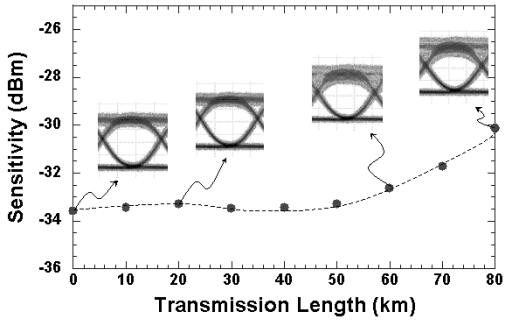

Fig. 10. Relation between the receiver sensitivity and the fiber transmission length for the carrier-suppressed DSB-SCM optical label signal.

section, a computer simulation is used to demonstrate the behavior of L; moreover, simulation and experimental results are presented to show that the small-signal approximation closely follows the behavior of DSB-SCM transmissions.

B. Experimental Demonstration and Simulations

An experiment was performed to show the influence of nonlinearities on DSB-SCM fading. Fig. 11 shows the experimental setup used, with greater detail of the DSB-SCM transmitter shown in Fig. 9. A Mach–Zehnder $LiNbO_3$ modulator with $\text{chirp parameter} = 0.4$ places the DSB-SCM transmitter output onto a 1550-nm wavelength, where the laser has been dithered to remove stimulated Brillouin scattering. This feeds into the propagation medium, a 20-km spool of standard SMF that, according to (8), will induce subcarrier suppression at frequencies close to 14 GHz. To precisely control the optical signal power P_{in} into the spool, an EDFA first amplifies the signal to greater than 20 dBm. The signal is then attenuated to the desired power using a variable attenuator. After propagation, a second EDFA serves as a preamp to the photodetector, but a second variable attenuator normalizes the received photodetector power to a constant level as P_{in} varies. Measured with the RF spectrum analyzer, the subcarrier frequency of the SCM-DSB transmitter was varied until it yielded minimum RF power due to fading. These null frequencies were measured

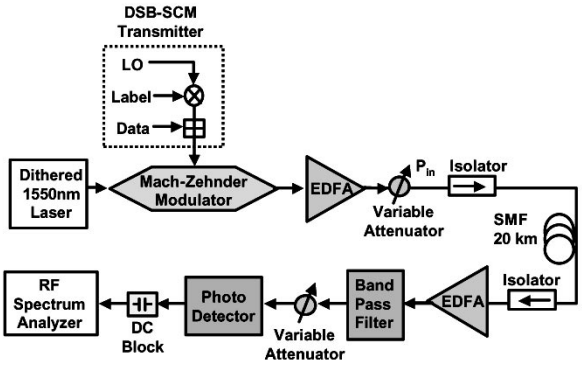

Fig. 11. Experimental setup for measuring DSB-SCM fading as a function of power.

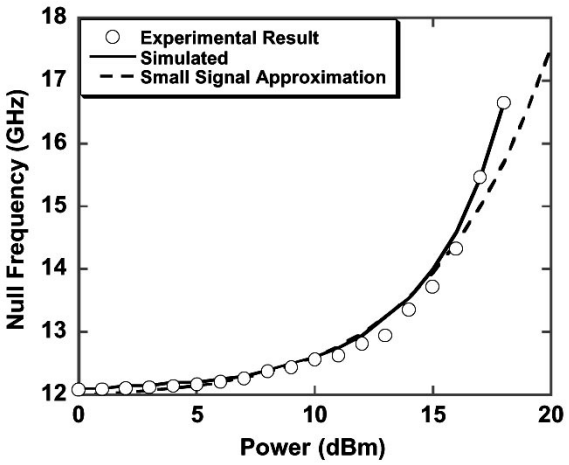

Fig. 12. DSB-SCM null frequencies as a function of power.

for increasing power levels, and Fig. 12 shows the results. It includes experimental data, a theoretical plot for (21), and simulated results of this experiment. The three are in excellent agreement with each other until higher order effects deviate them at very high power levels ($>$ 17 dBm). The equation closely follows the simulated and experimental results, showing that the small (modulation) signal approximation does not vary greatly from a true DSB-SCM transmission. All three results show that the subcarrier frequency remains virtually unchanged for powers below 5 dBm before beginning to increase.

To determine where subcarrier fading occurs as a function of distance and power, the simulation used for the set-up above propagated the light signal at varying fiber distances. The subcarrier frequency was kept fixed at 14 GHz, and instead of using an RF spectrum analyzer to measure the subcarrier power, an RF circuit filtered out the baseband signal, downshifted the subcarrier component, and obtained the BER of the label. Fig. 13 shows the simulator results; since the simulator uses an eye measurement to obtain the BER, it is able to obtain BERs smaller than 1E-15 and larger than 1E-1. Eye diagrams at 5 and 20 dBm show the progression of the eyes through 0, 15, and then every 20 km of fiber. The eyes degenerate where the BER is high, although the eyes at 20 dBm exhibit self-phase modulation even when the BER is low. The fiber distance where fading occurs increases as power increases; but more important, the fading range increases as well. The fading range is defined as the distances where fading causes poor BER performance, and clearly, this range is larger for 20 dBm than at 5 dBm. Thus, it becomes especially important to remove the fading effect when the fiber path includes fiber amplifiers, since the fading occurs over a much wider range of fiber distances.

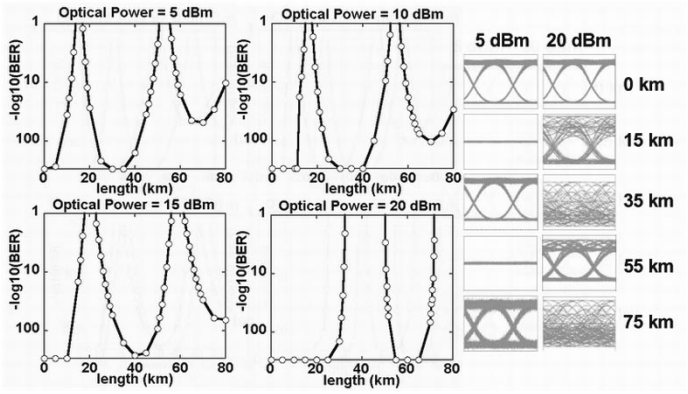

Fig. 13. Simulated behavior of subcarrier frequency with distance and power, with eye diagrams for 5 and 20 dBm at 0, 15, 35, 55, and 75 km.

V. All-Optical SCM Label Swapping

All-optical-label swapping is an important technology to provide scalability in OLS networks [8], [11]. As discussed in Section III, FBGs have the ability to separate the payload and the SCM label in optical domain, and this ability offers the possibility to achieve all-optical-label swapping. In the OLSR, an FBG extracts the labels optically and puts them into a label processor. The label processor generates new labels according to the old ones and modulates them onto an optical carrier. As Fig. 14 indicates, another FBG suppresses the optical carrier of this optical SCM carrying the new optical-label while the wavelength converter maps the data payload onto the same wavelength. Finally, a coupler combines the label and the payload and finishes the label-swapping operation. Experiments have successfully demonstrated error-free optical-label swapping with 2R data regeneration and without power penalty [26].

Fig. 14 shows the optical-label swapping module and the optical spectra at different points. The module consists of a DFB LD, a $LiNbO_3$ modulator, a 1×2 fiber coupler, two polarization controllers (PCs), a semiconductor optical amplifier-based Mach–Zehnder interferometer wavelength converter (SOA-based MZI WC), an isolator, an FBG, an EDFA, an attenuator, and a polarization beam combiner (PBC). Its top arm performs wavelength conversion of the payload, while the bottom arm performs SCM label rewriting. The DFB LD provides continuous-wave (CW) light to both arms through a 1×2 coupler. The signal light (inset (i) in Fig. 14) that goes into the SOA-based MZI WC only has the payload signal,

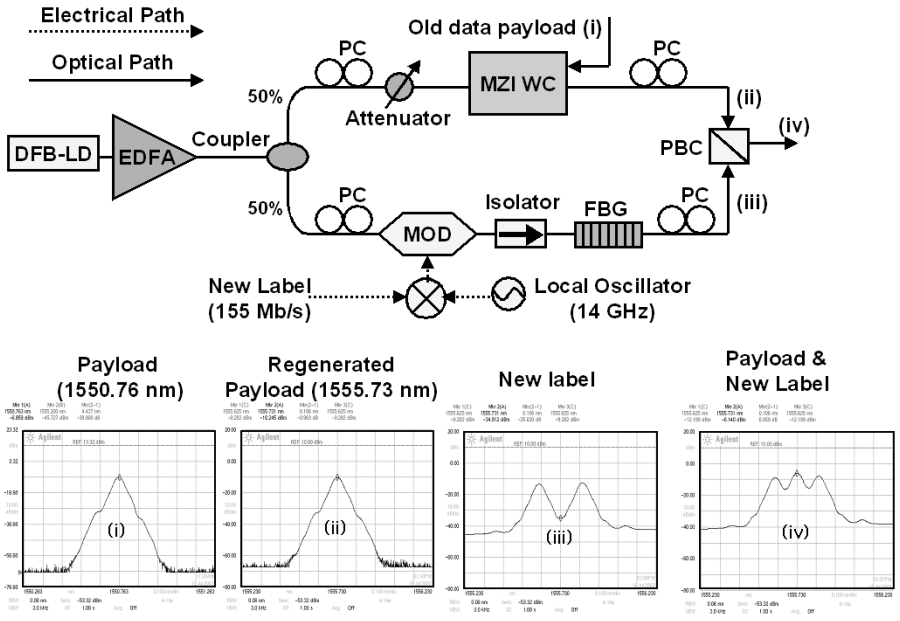

Fig. 14. Schematic diagram of the label swapping module. PC: polarization controller; MZI WC: Mach–Zehnder interferometer wavelength converter; FBG: fiber Bragg grating; Mod: modulator; PBC: polarization beam combiner. (Insets: (i) input payload (1550.76 nm), (ii) regenerated payload (1555.73 nm), (iii) new label, and (iv) regenerated DSB-SCM.)

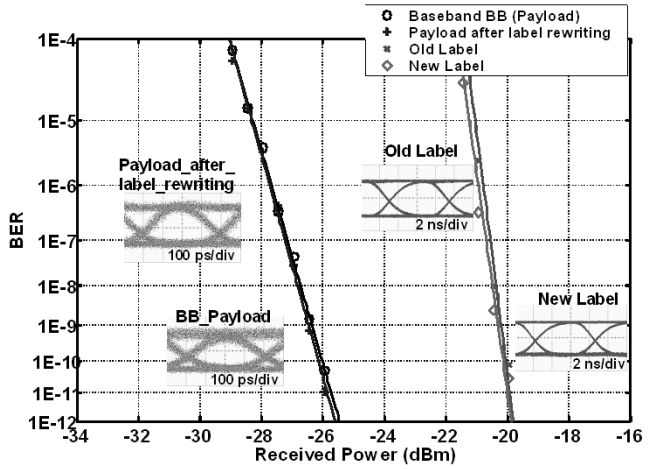

Fig. 15. BER test result for label swapping. (Insets: eye diagrams of the label and payload before and after label swapping.)

and its SCM label is already removed by an FBG. Then, the cross-phase modulation in the SOA-based MZI WC converts the payload signal onto the wavelength of the DFB LD (inset (ii) in Fig. 14). The new SCM label is modulated onto the light from the DFB LD by a $LiNbO_3$ modulator in the bottom arm. The FBG and the isolator suppress the optical carrier in the bottom arm and avoid interference with the payload (inset (iii) in Fig. 14). Finally, the PBC combines the payload and the new SCM label together (inset (iv) in Fig. 14). The purpose for using two PCs and a PBC here is to avoid undesired coherent interference between the two arms. Due to the finite extinction ratios of the FBG (approximately 25 dB), and there will be small but finite coherent interference if we use a conventional coupler.

BERs are measured on the label and the payload before and after the label swapping. Fig. 15 shows those BER results. The label swapping system imposes almost no power penalty to either the label or the payload. This is due to the 2R regeneration in the SOA-based MZI WC and the suppression of the intermodulation effect. These experimental results prove that SCM label swapping with simple system architecture and excellent performance is feasible, which is a prerequisite for cascadable OLS systems in a scalable network.

VI. Conclusion

This paper conducts theoretical and experimental investigations of linear and nonlinear optical studies on RF-photonics signal processing in optical subcarrier multiplexed systems. The signal processing normally conducted by using high-frequency RF electronics can be conducted by the optical filtering and low-frequency electronics. RF photonics signal processing also suppresses RF fading effects often seen in conventional RF DSB-SCM signal transmissions. The RF photonics signal processings applied to DSB and SSB subcarrier signals both show excellent performance. Theoretical and experimental results also indicate very good agreements for both linear and nonlinear optical processes in the fiber. Optical label swapping with RF photonics processing and 2R data regeneration indicate error-free performance for future applications in scalable optical-label switching networks.

References

[1] K. Fukuchi *et al.*, "10.92-Tb/s ($273 * 40$-Gb/s) triple-band/ultra-dense WDM optical-repeatered transmission experiment," in *Proc. OFC'2001*, vol. 4, Washington, DC, 2001, pp. PD24–1–PD24–3.

[2] S. J. B. Yoo, G. K. Chang, and Bellcore, U. S. A., "High-throughput, low-latency next generation Internet using optical tag switching," U. S. Patent 6 111 673, Aug. 29, 2000.
[3] S. J. B. Yoo *et al.*, "High-performance optical-label switching packet routers and smart edge routers for the next generation Internet," *IEEE J. Select. Areas Commun.*, pp. 1041–1051, Sept. 2003.
[4] S. F. Su, A. R. Bugos, V. Lanzisera, and R. Olshansky, "Demonstration of a multiple-access WDM network with subcarrier-multiplexed control channels," *IEEE Photon. Technol. Lett.*, vol. 6, pp. 461–463, Mar. 1994.
[5] C. Guillemot *et al.*, "Transparent optical packet switching: The European ACTS KEOPS project approach," *J. Lightwave Technol.*, vol. 16, pp. 2117–2134, Dec. 1998.
[6] C. Bintjas *et al.*, "All-optical packet address and payload separation," *IEEE Photon. Technol. Lett.*, vol. 14, pp. 1728–1730, Dec. 2002.
[7] O. Moriwaki, T. Sakamoto, A. Okada, and M. Matsuoka, "Optical packet switching using pattern-matching label processing based on an optical timing pulse generator," presented at the ECOC'02, Copenhagen, Denmark, Sept. 8–12, 2002, Paper 5.5.6.
[8] D. J. Blumenthal *et al.*, "All-optical label swapping networks and technologies," *J. Lightwave Technol.*, vol. 18, pp. 2058–2074, Dec. 2000.
[9] A. Okada, "All-optical packet routing in AWG-based wavelength routing networks using an out-of-band optical label," in *Proc. OFC'02*, vol. 1, Washington, DC, 2002, Paper WG1, pp. 213–215.
[10] N. Wada, H. Harai, W. Chujo, and F. Kubota, "Multi-hop, 40 Gbit/s variable length photonic packet routing based on multi-wavelength label switching, waveband routing, and label swapping," in *Proc. OFC'02*, vol. 1, Washington, DC, 2002, WG3, pp. 216–217.
[11] B. Meagher *et al.*, "Design and implementation of ultra-low latency optical label switching for packet-switched WDM networks," *J. Lightwave Technol.*, vol. 18, pp. 1978–1987, Dec. 2000.
[12] Y. M. Lin, W. I. Way, and G. K. Chang, "A novel optical label swapping technique using erasable optical single-sideband subcarrier label," *IEEE Photon. Technol. Lett.*, vol. 12, pp. 1088–1090, Aug. 2000.
[13] A. B. Sahin and A. E. Willner, "Dispersion division multiplexing for in-band subcarrier-header-based all-optical packet switching," in *Proc. OFC'02*, vol. 1, Washington, DC, 2002, Paper WO1, pp. 279–280.
[14] F. Devaux, Y. Sorel, and J. F. Kerdiles, "Simple measurement of fiber dispersion and of chirp parameter of intensity modulated light emitter," *J. Lightwave Technol.*, vol. 11, pp. 1937–1940, Dec. 1993.
[15] H. J. Lee, V. Hernandez, V. K. Tsui, and S. J. B. Yoo, "Simple, polarization-independent, and dispersion-insensitive SCM signal extraction technique for optical switching systems applications," *Electron. Lett.*, vol. 37, no. 20, pp. 1240–1241, Sept. 2001.
[16] E. Lallas, N. Skarmoutsos, and D. Syvridis, "A new all optical label swapping method based on optical FSK header encoding on the intensity modulated payload," presented at the ECOC'02, Copenhagen, Denmark, Sept. 8–12, 2002, Paper P4.4.
[17] J. Zhang, N. Chi, P. Holm-Nielsen, C. Peucheret, and P. Jeppesen, "A novel optical labeling scheme using a FSK modulated DFB laser integrated with an EA modulator," presented at the OFC'03, Atlanta, GA, Mar. 23–28, 2003, Paper TuQ5.
[18] N. Chi, L. Xu, L. Christiansen, K. Yvind, J. Zhang, P. Holm-Nielsen, C. Peucheret, C. Zhang, and P. Jeppesen, "Optical label swapping and packet transmission based on ASK/DPSK orthogonal modulation format in IP-over-WDM networks," presented at the OFC'03, Atlanta, GA, Mar. 23–28, 2003, FS2.
[19] E. N. Lallas, N. Skarmoutsos, and D. Syvridis, "An optical FSK-based label coding technique for the realization of the all-optical label swapping," *IEEE Photon. Technol. Lett.*, vol. 14, pp. 1472–1474, Oct. 2002.
[20] N. Chi *et al.*, "Dispersion management for two-level optically labeled signals in IP-over-WDM networks," presented at the ECOC'02, Copenhagen, Denmark, Sept. 8–12, 2002, Paper 5.5.1.
[21] T. Koonen *et al.*, "Optical labeling of packet in IP-over-WDM networks," presented at the ECOC'02, Copenhagen, Denmark, Sept. 8–12, 2002, Paper 5.5.2.
[22] M. Hickey and L. Kazovsky, "The STARNET coherent WDM computer communication network: Experimental transceiver employing a novel modulation format," *J. Lightwave Technol.*, vol. 6, pp. 876–884, May 1994.
[23] H. Schmuck, "Comparison of optical millimeter-wave system concepts with regard to chromatic dispersion," *Electron. Lett.*, vol. 31, no. 21, pp. 1848–1849, Oct. 1995.
[24] F. Devaux, Y. Sorel, and J. F. Kerdiles, "Simple measurement of fiber dispersion and of chirp parameter of intensity modulated light emitter," *J. Lightwave Technol.*, vol. 11, pp. 1937–1940, Dec. 1993.
[25] S. J. B. Yoo *et al.*, "Optical-label based packet routing system with contention resolution in wavelength, time, and space domains," in *Proc. OFC'02*, vol. 1, Washington, DC, 2002, Paper WO2, pp. 280–282.
[26] M. Jeon, Z. Pan, J. Cao, and S. J. B. Yoo, "All-optical sub-carrier label swapping with 2R regeneration," presented at the OFC'03, Atlanta, GA, Mar. 23–28, 2003, Paper TuQ4.
[27] J. Cao *et al.*, "Error-free multi-hop cascaded operation of optical label switching routers with all-optical label swapping," presented at the OFC'03, Atlanta, GA, Mar. 23–28, 2003, Paper FS1.
[28] N. Chi, L. Xu, L. Christiansen, K. Yvind, J. Zhang, P. Holm-Nielsen, C. Peucheret, C. Zhang, and P. Jeppesen, "Optical label swapping and packet transmission based on ASK/DPSK orthogonal modulation format in IP-over-WDM networks," presented at the OFC'03, Atlanta, GA, Mar. 23–28, 2003, Paper FS2.
[29] R. Rawaswami and K. Sivarajan, *Optical Networks: A Practical Perspective*. San Mateo, CA: Morgan Kaufmann, 2002.
[30] Y. M. Lin, W. I. Way, and G. K. Chang, "A novel optical label swapping technique using erasable optical single-sideband subcarrier label," *IEEE Photon. Technol. Lett.*, vol. 12, pp. 1088–1090, Aug. 2000.

Zuqing Zhu (S'03) received the B.S. degree from the Department of Electronic Engineering and Information Science, University of Science and Technology of China, Hefei, China, in 2001 and the M.S. degree from the Department of Electrical and Computer Engineering, University of California, Davis, in 2003. He is currently working toward the Ph.D. degree at the Department of Electrical and Computer Engineering, University of California, Davis.

His research focuses on advanced switching technologies and optical communication systems for the next-generation optical networks.

Mr. Zhu is a Student Member of the Optical Society of America (OSA).

V. J. Hernandez was born in San Francisco, CA, on December 9, 1976. He received the B.S. degree in electrical engineering from the University of California, Davis, in 1999. He is currently working toward the Ph.D. degree in electrical engineering at the University of California, Davis.

He is a student employee at Lawrence Livermore National Laboratory. His interests include optical label switching technologies for optical networks, ultrashort-pulse optical-code-division multiplexing access (OCDMA), and matrix-coding direct sequence OCDMA networks.

Min Yong Jeon received the B.S. degree from Han Yang University, Seoul, Korea, in 1988 and the M.S. and Ph.D. degrees from Korea Advanced Institute of Science and Technology (KAIST), Daejeon, Korea, in 1990 and 1994, respectively, all in physics.

Prior to joining Chung Nam University, he worked in the area of optical routers, as a Research Scientist at the University of California, Davis. From 1994 to 2001, he worked in the area of the optical network subsystems at the Electronics and Telecommunications Research Institute (ETRI), Daejeon, Korea. He has been with the Chung Nam National University, Daejeon, Korea, as an Assistant Professor of Physics since May 2003. His current research interests include characterization and application of optical switching technologies, amplifiers, lasers and optical nonlinear effects.

Prof. Jeon is a Member of the Optical Society of America (OSA).

Jing Cao (S'03) received the B.S. and M.S. degrees from the Department of Electronics Engineering, Tsinghua University, Beijing, China, in 1997 and 2000, respectively, and is working toward the Ph.D. degree at the Electrical and Computer Engineering Department, University of California, Davis.

His research focuses on optical integrated devices and system integration for next-generation optical networks.

Mr. Cao is a Student Member of the Optical Society of America (OSA).

Zhong Pan (S'03) received the B.S. degree from the Department of Electronic Engineering, Tsinghua University, Beijing, China, in 2000 and the M.S. degree from the Department of Electrical and Computer Engineering, University of California, Davis, in 2002. He is currently working toward the Ph.D. degree at the University of California, Davis.

His research focuses on optical-label switching in optical communication networks, especially the control of the tunable laser and its application.

Mr. Pan is a Student Member of the Optical Society of America (OSA).

S. J. Ben Yoo (S82–M'84–SM'97) received the B.S. degree in electrical engineering with distinction, the M.S. degree in electrical engineering, and the Ph.D. degree in electrical engineering with a minor degree in physics from Stanford University, Stanford, CA, in 1984, 1986, and 1991, respectively. His Ph.D. thesis was on linear and nonlinear optical spectroscopy of quantum-well intersubband transitions.

Prior to joining Bellcore in 1991, he conducted research on nonlinear optical processes in quantum wells, a four-wave-mixing study of relaxation mechanisms in dye molecules, and ultrafast diffusion driven photodetectors. During this period, he also conducted research on lifetime measurements of intersubband transitions and on nonlinear optical storage mechanisms at Bell Laboratories and IBM Research Laboratories, respectively. He was then a Senior Scientist at Bellcore, leading technical efforts in optical networking research and systems integration. His research activities at Bellcore included optical-label switching for the Next Generation Internet, power transients in reconfigurable optical networks, wavelength interchanging cross-connects, wavelength converters, vertical-cavity lasers, and high-speed modulators. He also participated in the Advanced Technology Demonstration Network and Multiwavelength Optical Networking (ATD/MONET) systems integration, the OC-192 synchronous optical network (SONET) ring studies, and a number of standardization activities. He joined the University of California, Davis (UC Davis), as Associate Professor of Electrical and Computer Engineering in March 1999. He is currently Professor and the Branch Director of the Center for Information Technology Research in the Interest of Society (CITRIS). His current research involves advanced switching techniques and optical communications systems for the Next Generation Internet. In particular, he is conducting research on architectures, systems integration, and network experiments of all-optical label switching routers.

Prof. Yoo is an Associate Editor for the IEEE PHOTONICS TECHNOLOGY LETTER, a Senior Member of IEEE Lasers & Electro-Optics Society (LEOS) and a Member of the Optical Society of America (OSA) and Tau Beta Pi. He received the Bellcore CEO Award in 1998 and DARPA Award for Sustained Excellence in 1997 for his work at Bellcore.